Ligand-Stabilized Reduced-Dimensionality Perovskites

Supporting Information

Li Na Quan,[1,2]† Mingjian Yuan,[1]† Riccardo Comin,[1] Oleksandr Voznyy,[1] Eric M. Beauregard,[1] Sjoerd Hoogland,[1] Andrei Buin,[1] Ahmad R. Kirmani,[3] Kui Zhao,[3] Aram Amassian,[3] Dong Ha Kim,[2*] Edward H. Sargent[1*]

[1] Department of Electrical and Computer Engineering, University of Toronto, 10 King's College Road, Toronto, Ontario, M5S 3G4, Canada

[2] Department of Chemistry and Nano Science, Ewha Womans University, 52, Ewhayeodae-gil, Seodaemun-gu, Seoul 03760, Korea

[3] Solar and Photovoltaic Engineering Research Center, King Abdullah University of Science and Technology (KAUST), Thuwal 23955-6900, Saudi Arabia

† These authors contributed equally to this work.

[*] E-mail: ted.sargent@utoronto.ca (EHS); dhkim@ewha.ac.kr (DHK)

1. Details for Density functional theory Simulations for the perovskite stability.

1.1 Methods

Calculations were performed using the Quickstep module of the CP2K program suite[S1,S2] utilizing a combined basis of Gaussians and plane waves, using Perdew–Burke–Ernzerhof (PBE) exchange correlation functional. A grid cutoff of 300 Ry was used, appropriate for the Goedecker–Teter–Hutter pseudopotentials[S3] that we employed. Triple-zeta plus polarization (TZVP) basis sets for H, C, N and double-zeta (DZVP) for Pb and I were used[S4]. Basis set superposition error corrections were applied to all binding energy calculations using the counterpoise method ('ghost' neighboring atomic orbitals). Van der Waals interactions were included as empirical dispersion corrections[S5]. Simulations were performed using periodic boundary conditions on slabs ranging from 1 to 40 layers in a 3x3 tetragonal perovskite surface unit cell (26x26 $Å^2$) using a single k-point. Perovskite layers were stacked on top of each other along the crystallographic *c*-axis. Full structural and cell optimization was performed for each structure using Broyden-Fletcher-Goldfarb-Shanno algorithm (BFGS).

1.2 Results and Discussion

Formation energies were calculated as follows:

$$E = \frac{E_{(\mathrm{PbI_2})_n(\mathrm{MAI})_{n-1}(\mathrm{PEAI})_2} - nE_{\mathrm{PbI_2}} - (n-1)E_{MAI} - 2E_{PEAI}}{n}$$

with negative values meaning stable structure. The PbI_2 energy is taken to be that of bulk. MAI and PEAI energies were computed for bulk MAI and PEAI, as well as gas phase and solvated with different amounts of water, increasing the stability of molecules and thus decreasing the stability of perovskite (fig. S1b and c). Desorption into $HI+CH_3NH_2$ was also considered but had higher energy cost.

Perovskite formation energy vs. decomposition into bulk constituents is found to be 0.05 eV with van der Waals interactions included, and -0.1 eV when omitted. The exact value of the formation energy depends on the exchange-correlation potential used[S6] but is expected to be close to zero irrespectively, *i.e.* indicating intrinsic poor stability of the perovskite.

To decompose the formation enthalpy into contributions from MAI and PbI_2, slabs of different thicknesses were used: PEAI, PbI_2, and MAI layers were successively removed and compared to energies of the bulk PEAI, PbI_2, and MAI. These layer desorption energies were found to be independent of the amount of layers (*n*) in the slab and comprise 0.55 eV per molecule for MAI, 0.91 eV for PEAI, and -0.6 eV for PbI_2 (positive value means stable).

MAI and PEAI desorption energies with and without van der Waals contribution were compared, and the difference of 0.36 eV was found to be completely caused by van der Waals interactions, irrespective of the environment (humidity). To account for the possibility of imperfect surface coverage by PEAI, especially for the cases of high *n* values where excess of MAI is significant, intermixed 1:1 MAI:PEAI surface layer was modeled, leading to a 0.18 eV per molecule reduction in surface layer desorption energy.

Obtained energies for desorption from perovskite into gas phase are 2.15 and 2.51 eV, for MAI and PEAI respectively, rendering perovskite stable under vacuum. Desorption into water is found to be comparable to decomposition into bulk MAI/PEAI; while lower humidity, corresponding to less water molecules used in simulation, improves the stability by 0.35 eV (for the configuration in Fig. S1c).

To estimate the film decomposition lifetime for Fig.1b, we follow the methodology for surface thermal desorption spectroscopy, where molecular desorption rate *r* is given by:

$$r = -\frac{d\sigma}{dt} = \nu \exp(-\frac{E_a}{kT}),$$

where σ is the surface coverage, ν – attempt frequency, E_a – activation energy. The film decomposition lifetime is then given by:

$$t = N_{MAI} / r_{MAI} + N_{PEAI}/r_{PEAI.}$$

where *N* is the amount of the respective molecules in the film. We estimate *N* by assuming a film thickness of 400 nm and a thickness of 0.6 nm per PbI_2+MAI layer for Fig.1b.

Since v is unknown a priori, we use relative rates, which are fully defined by the energy difference between the respective activation energies. For example, 0.36 eV stabilization of PEAI relative to MAI provides six orders of magnitude slower rate. Combined with ~700 MAI layers in a 400 nm film, this leads to about three orders of magnitude longer decomposition lifetime in case of a single PEAI protective surface layer (i.e. quasi-2D perovskite with n=700) fully covering the $MAPbI_3$ perovskite unit cell.

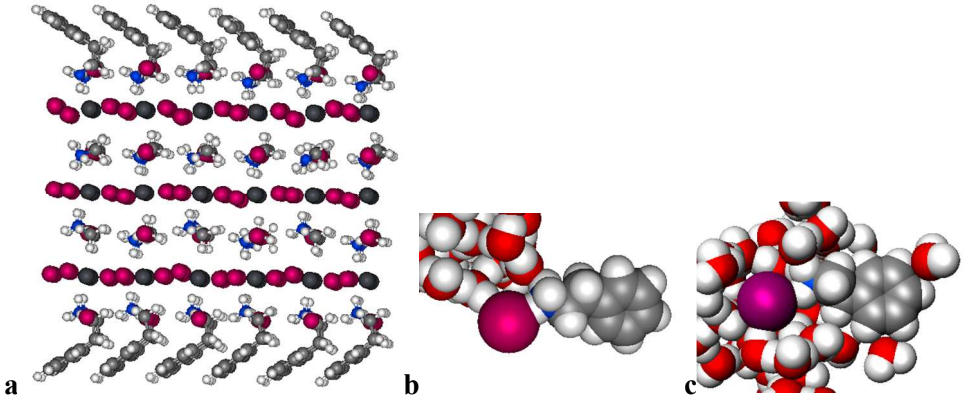

Figure S1. Geometries used in DFT simulations. a, Example of a unit cell for the perovskite with $n=3$. b, PEAI near water cluster. c, PEAI in bulk water. Atom color legend: black–lead; purple –iodine; grey – carbon; red –oxygen; white –hydrogen.

2. Optoelectronic device simulations using SCAPS 3.0.01.

Optoelectronic simulations were performed using SCAPS 3.0.01 modeling program[S6, S7]. Gold and ITO work functions were used for contacts, with TiO_2 electron transport layer (Electron Affinity EA=4.1 eV) and Spiro-OMeTAD (ionization potential IP=5.3 eV) hole transport layer explicitly included. A perovskite layer thickness of 400 nm was used, EA of 3.9 eV, and taking the absorption spectra and bandgaps for different *n*-layers from experimental measurements. Neutral defects were introduced 0.5 eV below the conduction band of perovskite (green line in Fig. S2) as a single effective level, with trap density and capture cross-section density adjusted to achieve the experimentally observed diffusion length of ~350 nm.

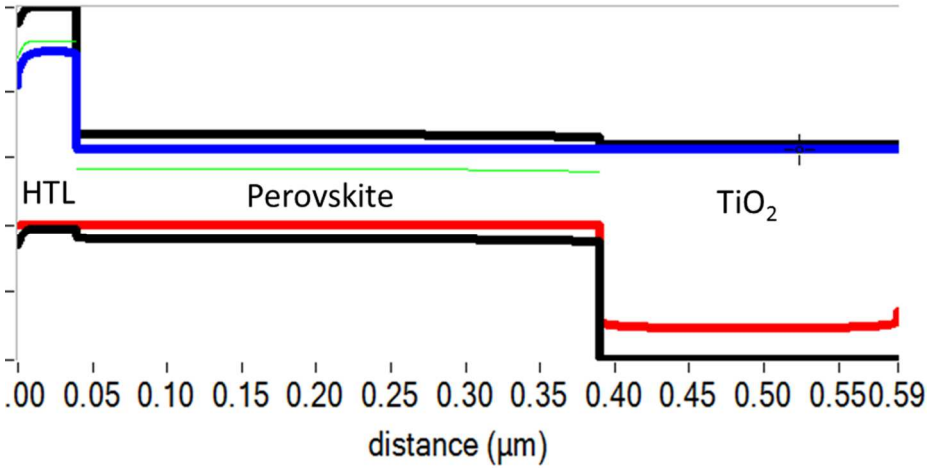

Figure S2. Simulated band diagram of the perovskite device at V_{OC}.

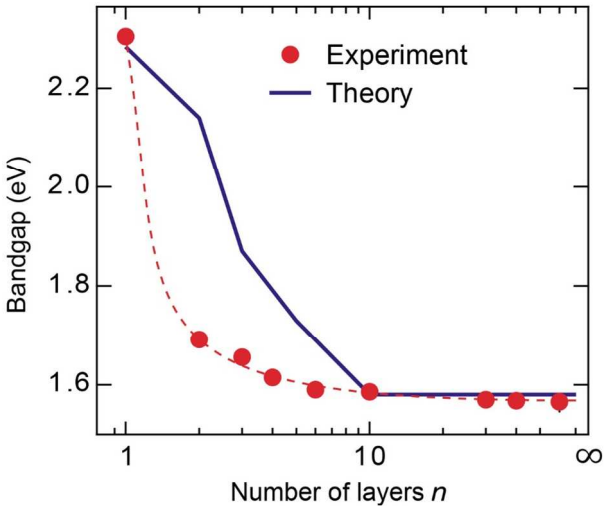

Figure S3. Experimental absorption band edge (from the absorption onset, solid line) and DFT simulated absorption band edge of perovskite with different *n* values (dashed red line is guide to the eye).

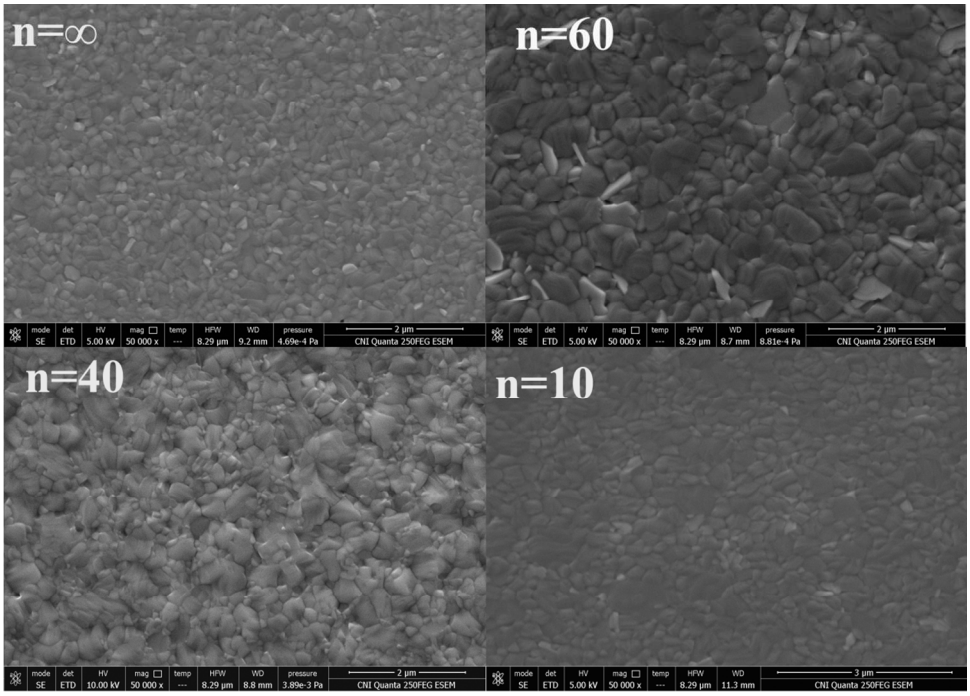

Figure S4. Top-View SEM images of the perovskite films with different *n* values using solvent engineering technique.

Newport	ACCREDITED Calibration Cert. # 2893.01	Technology and Application Center **PV Lab** Newport Calibration Cert. # 1255

DUT S/N: L48
Newport Calibration #: 1255
Manufacturer: University of Toronto, Dept. of ECE, Ted Sargent Group
Material: Perovskite
Temperature Sensor: TC-K
Environmental conditions at the time of calibration: Temperature: 24 ± 3 °C; Humidity: 40 ± 10 %

The above DUT has been tested using the following methods to meet the ISO 17025 Standard by the PV Lab at Newport Corporation. Quoted uncertainties are expanded using a coverage factor of $k = 2$ and expressed with an approximately 95% level of confidence. Measurement of total irradiance is traceable to the World Radiometric Reference (WRR) and all other measurements and uncertainties are traceable to either NIST or CNRC and the International System of Units (SI). The performance parameters reported in this certificate apply only at the time of the test, and do not imply future performance.

Efficency [%]	15.29	±	0.34	V_oc [V]	1.0953	±	0.0152	I_sc [A]	0.000941	±	0.000017
P_max [mW]	0.759	±	0.016	V_max [V]	0.9156	±	0.0099	I_max [A]	0.000829	±	0.000010
FF [%]	73.7	±	1.1	Area [cm^2]	0.0496	±	0.0002	M	0.996	±	0.004

Methods:

I-V: ASTM E948-15 *Standard Test Method for Electrical Performance of Photovoltaic Cells Using Reference Cells Under Simulated Sunlight*
QE: ASTM E1021-15 *Standard Test Method for Spectral Responsivity Measurements of Photovoltaic Devices*

Standard Reporting Conditions:

Spectrum: AM1.5-G (ASTM G173-03/IEC 60904-3 ed. 2)
1000.0 W/m ^{2} at 25.0°C

Secondary Reference Cell:

Device S/N: PVM 284 KG5
Device Material: mono-Si
Window Material: KG5
Certification: National Renewable Energy Laboratory
A2LA accreditation certificate # 2236.01
ISO Tracking #: 1811
Certified short circuit current (I_{sc}) under standard reporting conditions (SRC): 33.803mA
Calibration due date: 11-Aug-15

Solar Simulator:

Spectrum: Newport Corporation filename *Sol3A_Spectroradiometer_Scan_0171.xls*
Total irradiance: 1000 W/m^2 based on I_{sc} of the above Secondary Reference Cell

Quantum Efficiency for DUT:

Newport Corporation filename *QE 1255 L48.xls*
Spectral mismatch correction factor: M = 0.996 ± 0.004

DUT Calibration Procedures:

Newport Corporation document WI1 (EQE).docx
Newport Corporation document Area Measurement WI2 (Area).docx
Newport Corporation document WI3 (IV.Sweep).docx

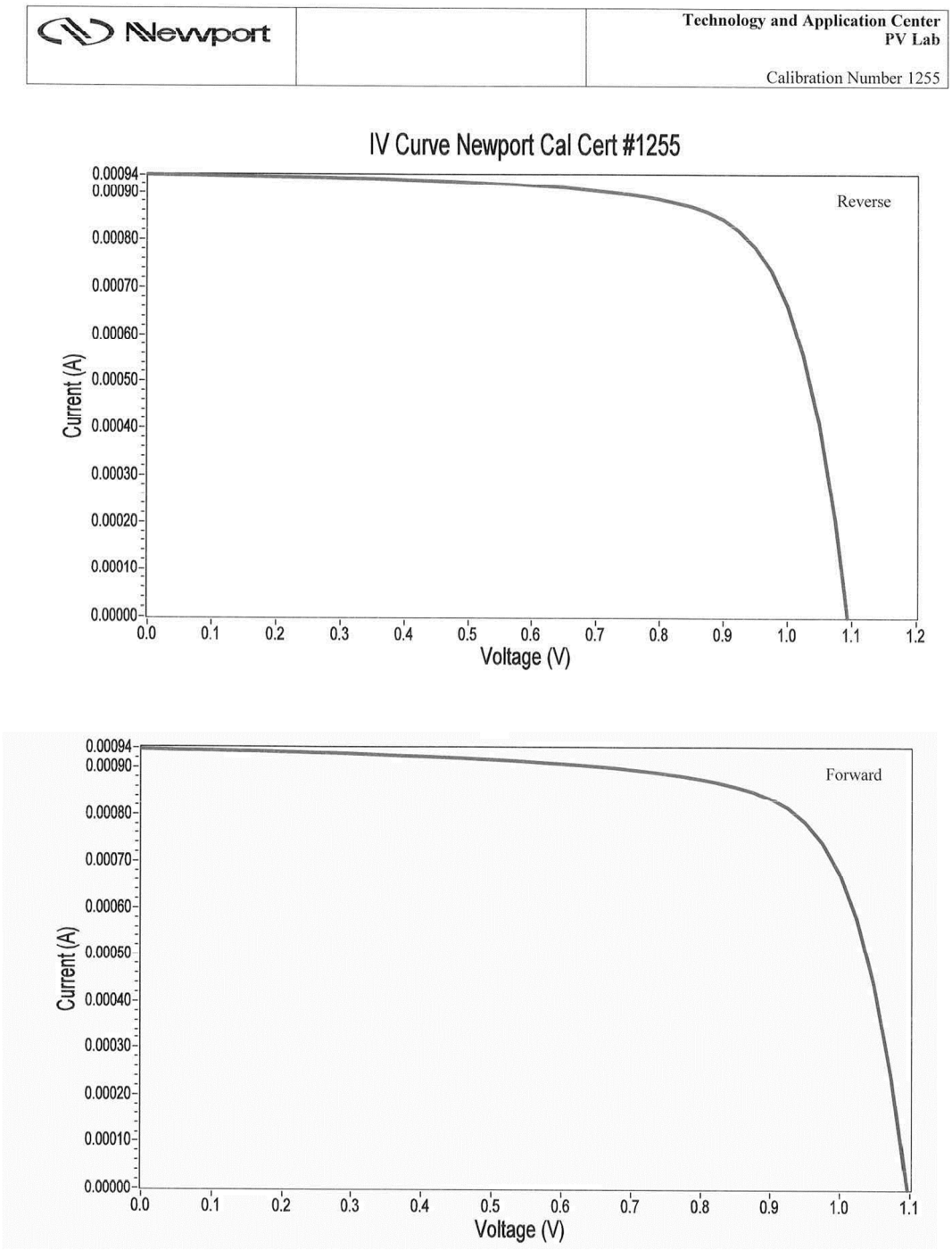

Figure S5. Independent certification from photovoltaic calibration laboratory in Newport Technology and Application Center–PV Lab.

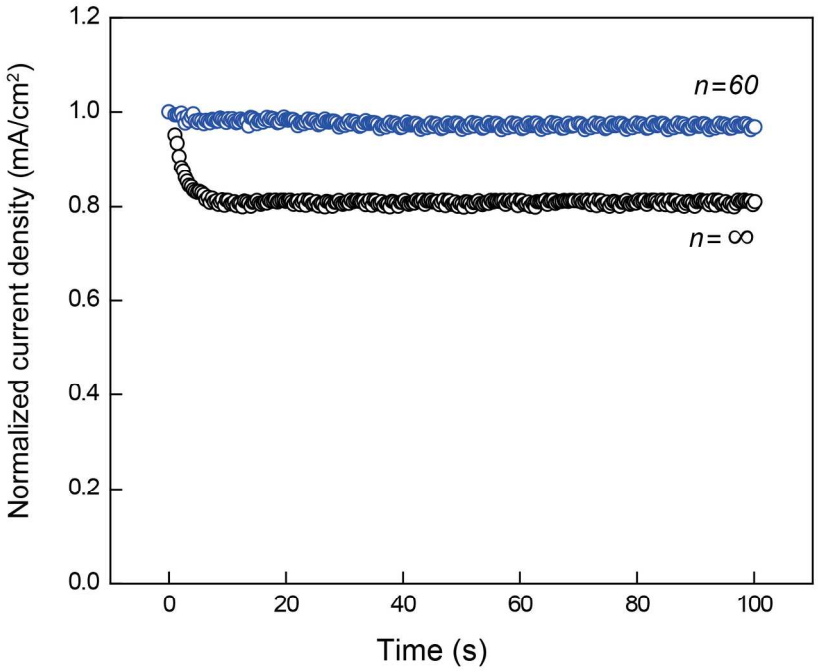

Figure S6. Steady state current density measurement at the maximum current density of devices using $n = \infty$ and $n = 60$ devices. The stable current output at maximum point indicates no hysteresis.

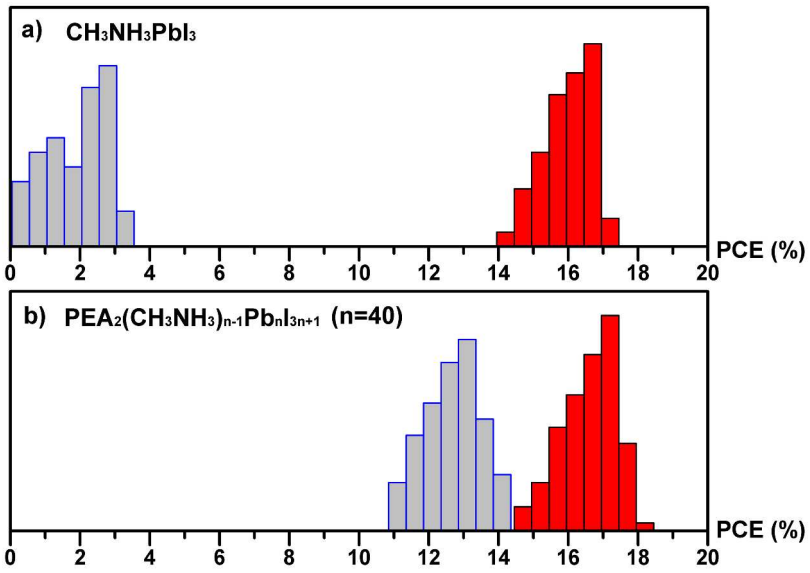

Figure S7. The evolution of device performance distribution histograms, red column represents the initial device performance distribution, grey column represents the device performance distribution after 1440 hrs (60 days). a) Traditional 3D perovskite; b) quasi-2D perovskite, with n = 40.

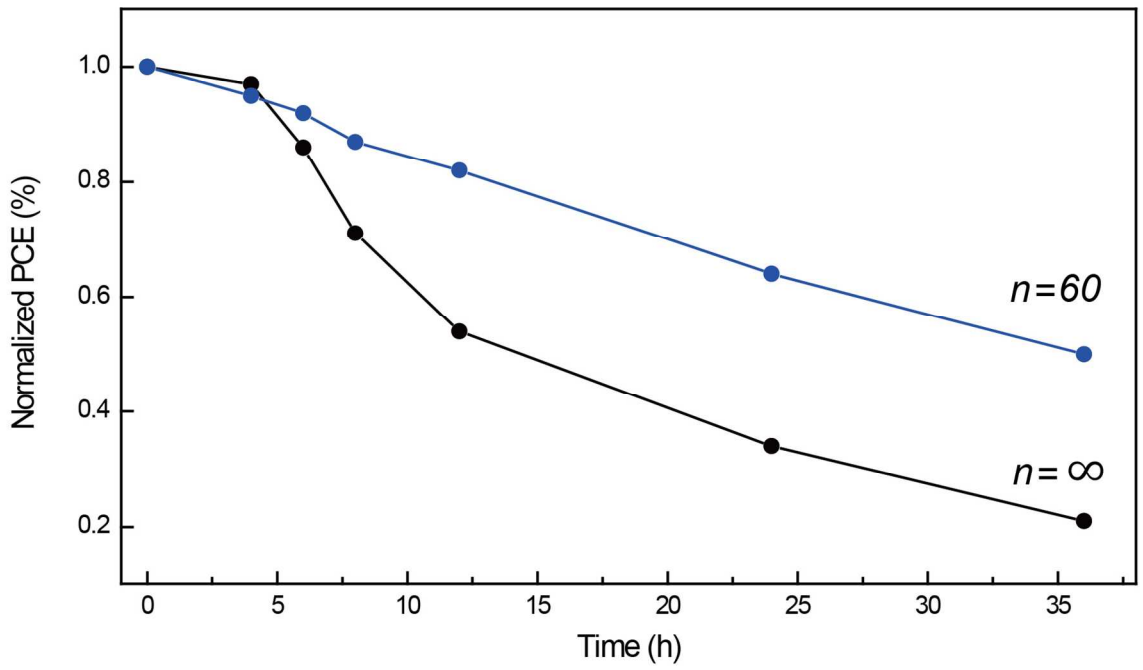

Figure S8. Thermal stability of $\boldsymbol{n = \infty}$ and $\boldsymbol{n = 60}$ devices after annealing under 100°C in nitrogen filled glove box for 36 hr.

Table S1. The molecular formula for perovskite with different *n* values and the amount of each precursor for preparing the resulting films.

n	Molecular formula	PbI_2 concentration	MAI concentration	PEAI concentration
1	$(PEA)_2PbI_4$	2.05 mmol/ ml (945.05 mg/ml)	0	4.1 mmol/ml (1020.9 mg/ml)
6	$(PEA)_2(MA)_5Pb_6I_{19}$	2.05 mmol/ ml (945.05 mg/ml)	1.71 mmol/ml (271.6 mg/ml)	0.68 mmol/ml (170.2 mg/ml)
10	$(PEA)_2(MA)_9Pb_{10}I_{31}$	2.05 mmol/ ml (945.05 mg/ml)	1.85 mmol/ml (293.4 mg/ml)	0.41 mmol/ml (102.1 mg/ml)
40	$(PEA)_2(MA)_{39}Pb_{40}I_{121}$	2.05 mmol/ ml (945.05 mg/ml)	2.00 mmol/ml (317.8 mg/ml)	0.103 mmol/ml (25.5 mg/ml)
60	$(PEA)_2(MA)_{59}Pb_{60}I_{181}$	2.05 mmol/ ml (945.05 mg/ml)	2.02 mmol/ml (320.5 mg/ml)	0.068 mmol/ml (17.1 mg/ml)
∞	$MAPbI_3$	2.05 mmol/ ml (945.05 mg/ml)	2.05 mmol/ ml (326.0 mg/ml)	0

Table S2. Measured diffusion length for perovskite material with different *n* values. The measurement was carried out following the published procedure.

n values	L_D
n=∞	515.82 nm
n=60	764.45 nm
n=40	378.32 nm
n=10	357.07 nm

Table S3. Summary of champion perovskite device for different *n* values.

n	V_{oc}	J_{sc}	FF	PCE (Champion)
∞	1.03 V	22.00 mA/cm^2	76.10%	17.24%
60	1.06 V	22.45 mA/cm^2	77.30%	18.40%
40	1.09 V	22.56 mA/cm^2	74.20%	18.24%
30	1.11 V	20.34 mA/cm^2	72.37%	16.34%
20	1.12 V	20.31 mA/cm^2	69.41%	15.79%
10	1.16 V	18.66 mA/cm^2	64.40%	13.89%
6	1.15 V	18.23 mA/cm^2	44.00%	9.22%

Table S4. Record of J_{sc} change for different perovskite device stored in Nitrogen over two months.

J_{sc}	Initial	1 week	4 weeks	8 weeks
n=∞	20.89 mA/cm^2	19.54 mA/cm^2	17.24 mA/cm^2	10.69 mA/cm^2
n=60	21.83 mA/cm^2	20.76 mA/cm^2	19.03 mA/cm^2	17.92 mA/cm^2
n=40	21.48 mA/cm^2	21.05 mA/cm^2	19.42 mA/cm^2	18.54 mA/cm^2
n=10	19.41 mA/cm^2	19.38 mA/cm^2	19.30 mA/cm^2	19.16 mA/cm^2

Table S5. Record of PCE change for different perovskite device stored in Nitrogen over two months.

PCE	Initial	1 week	4 weeks	8 weeks
n=∞	16.69%	12.51%	7.01%	2.80%
n=60	17.59%	16.16%	13.89%	11.34%
n=40	17.34%	16.47%	15.19%	13.11%
n=10	12.77%	12.07%	11.93%	10.92%

Table S6. Record of V_{oc} change for different perovskite device stored in Nitrogen over two months.

V_{oc}	Initial	1 week	4 weeks	8 weeks
$n = \infty$	1.05 V	1.04 V	0.90 V	0.88 V
$n = 60$	1.07 V	1.07 V	1.06 V	1.02 V
$n = 40$	1.10 V	1.09 V	1.09 V	1.06 V
$n = 10$	1.12 V	1.11 V	1.11 V	1.10 V

Table S7. Record of FF change for different perovskite device stored in Nitrogen over two months.

FF	Initial	1 week	4 weeks	8 weeks
$n=\infty$	76.09%	61.55%	45.20%	29.78%
$n=60$	75.32%	72.74%	68.87%	62.02%
$n=40$	73.40%	71.80%	71.76%	66.72%
$n=10$	58.72%	56.10%	55.71%	51.83%

Table S8. Record of PCE change for different perovskite device stored in humidity air (RH 55%) over two weeks.

PCE	Initial	1 day	3 days	7 days	14 days
$n = \infty$	16.47%	7.64%	4.23%	0.93%	0.72%
$n = 60$	17.21%	17.03%	15.34%	14.09%	12.80%
$n = 40$	17.10%	17.10%	16.52%	15.13%	13.14%
$n = 10$	13.20%	13.23%	12.69%	12.04%	11.47%

References:

S1. Perdew, J. P.; Burke, K.; Ernzerhof, M. *Phys. Rev. Lett.* **1996**, **77**, 3865.

S2. Vondele V, J.; Krack, M.; Mohamed, F.; Parrinello, M.; Chassaing, T.; Hutter, J. *J. Comp. Phys. Comm.* **2005**, 167, 103-128.

S3. Hartwigsen, C.; Goedecker, S.; Hutter, J. *Phys. Rev. B* **1998**, 58, 3641.

S4. Vondele V, J.; Hutter, J. *J. Chem. Phys*. **2007**, 127, 114105.

S5. Grimme, S.; Antony, J.; Ehrlich, S.; Krieg, H. *J. Chem. Phys.* **2010**, 132, 154104.

S6. Burgelman, M.; Nollet, P.; Degrave, S. *Thin Solid Film* **2000**, 527, *361*.

S7. Burgelman, M.; Verschraegen, J.; Degrave, S.; Nollet, P. *Prog. Photovolt: Res. Appl*. **2004**, 12, 143-147.